ASME 2012 5th Annual Dynamic Systems and Control Conference joint with the
JSME 2012 11th Motion and Vibration Conference
DSCC2012-MOVIC2012
October 17-19, 2012, Fort Lauderdale, Florida, USA

DSCC2012-MOVIC2012-8580

BROADBAND DISTURBANCE REJECTION USING RETROSPECTIVE COST ADAPTIVE CONTROL

E. Dogan Sumer
Department of Aerospace Engineering
University of Michigan
Ann Arbor, Michigan 48109-2140
Email: dogan@umich.edu

Jesse B. Hoagg
Mechanical Engineering Department
University of Kentucky
Lexington, Kentucky, 40506-0503
jhoagg@engt.uky.edu

Dennis S. Bernstein
Department of Aerospace Engineering
University of Michigan
Ann Arbor, Michigan 48109-2140
Email: dsbaero@umich.edu

ABSTRACT

We apply retrospective cost adaptive control (RCAC) to a broadband disturbance rejection problem under limited modeling information and assuming that the performance variable is measured. The goal is to compare the asymptotic performance (that is, after convergence of the controller) of the adaptive controller with the performance of discrete-time LQG controller, which uses complete modeling information but does not require a measurement of the performance variable. For RCAC we assume that the first nonzero Markov parameter of the plant is known. We show that if the plant zeros are also known, the retrospective cost can be modified to recover the high-control-authority LQG performance.

1 INTRODUCTION

The goal of robust control is to design controllers that account for prior uncertainty in the plant model. Robust control thus trades performance for uncertainty. In contrast, the goal of adaptive control is to avoid the need to sacrifice performance for modeling uncertainty by modifying the controller online to the actual plant. Adaptive control remains an active area of research [1, 2].

A common application of adaptive control is to command-following problems, where the goal is to have the plant follow an exogenous signal that is specified at the present time. This problem is usually cast in terms of model reference adaptive control [3–6].

For control applications requiring disturbance rejection, adaptive feedforward control algorithms such as filtered-X LMS have been developed [7]. These algorithms do not require knowledge of the disturbance spectrum, but require a direct measurement of the disturbance signal. For applications in which measurements of only the plant response are available, feedback control is needed. For systems with harmonic disturbances having known spectrum, such as active noise and vibration control in helicopters, harmonic steady-state algorithms can be used [8]. For disturbance rejection in the presence of harmonic disturbances with unknown spectra, adaptive feedback control methods have been developed [9–12].

A more challenging problem is adaptive disturbance rejection without feedforward measurements in the presence of broadband disturbances. For nonadaptive control with complete modeling information, LQG control can be used; for robust control, extensions to H_∞ are available [13]. Within the context of adaptive feedback control, adaptive LQG control is considered in [14, 15].

In the present paper we consider the adaptive broadband disturbance rejection using retrospective cost adaptive control (RCAC) [11, 12, 16, 17]. Although broadband disturbance rejection was demonstrated in [11, 12, 16], no attempt was made to compare the asymptotic performance of the adaptive controller under limited modeling information with the performance of LQG under complete modeling information. This is the goal of the present paper.

To compare the performance of RCAC with LQG, we consider a disturbance rejection problem in which the error signal is the input to the controller. This assumption is for convenience only since RCAC allows distinct error and measurement signals, as in the construction of the LQG cost. In the case where the performance variable does not coincide with the measurements, RCAC requires a measurement of the performance variable, which is not needed by LQG. The possible need for additional measurements by adaptive control reflects the tradeoff

between sensor hardware and modeling. As in [11, 12, 16–18], RCAC requires limited modeling information, specifically, Markov parameters from the control input to the error signal. The required accuracy of the Markov parameters, which drives the requirements for system identification, is discussed in [19].

2 BROADBAND DISTURBANCE REJECTION PROBLEM

Consider the discrete-time plant

$$x(k+1) = Ax(k) + Bu(k) + D_1 w(k), \tag{1}$$

where $k \geq 0$, $x(k) \in \mathbb{R}^n$, $u(k) \in \mathbb{R}^{l_u}$, $w(k) \in \mathbb{R}^{l_w}$ is zero-mean Gaussian white noise, and (A,B), (A,D_1) are stabilizable. Furthermore, let

$$y(k) = Cx(k) + D_2 w(k), \tag{2}$$
$$z(k) = E_1 x(k) + E_2 u(k), \tag{3}$$

where $y(k) \in \mathbb{R}^{l_y}$ is the output measurement vector, $z(k) \in \mathbb{R}^{l_z}$ is the performance variable that we desire to minimize, and (A,C), (A,E_1) are detectable. The plant (1)–(3) is described by

$$\begin{bmatrix} z \\ y \end{bmatrix} = G(z) \begin{bmatrix} w \\ u \end{bmatrix},$$

where

$$G(z) = \begin{bmatrix} G_{zw}(z) & G_{zu}(z) \\ G_{yw}(z) & G_{yu}(z) \end{bmatrix}$$

and

$$G_{zw}(z) = E_1(zI - A)^{-1} D_1, \tag{4}$$
$$G_{zu}(z) = E_1(zI - A)^{-1} B + E_2, \tag{5}$$
$$G_{yw}(z) = C(zI - A)^{-1} D_1 + D_2, \tag{6}$$
$$G_{yu}(z) = C(zI - A)^{-1} B. \tag{7}$$

Furthermore, the characteristic polynomial of the plant is

$$\mathcal{D}(z) \triangleq \det(zI - A). \tag{8}$$

Consider the $n_{\mathrm{c}}^{\mathrm{th}}$-order strictly proper output feedback controller

$$x_{\mathrm{c}}(k+1) = A_{\mathrm{c}} x_{\mathrm{c}}(k) + B_{\mathrm{c}} y(k), \tag{9}$$
$$u(k) = C_{\mathrm{c}} x_{\mathrm{c}}(k), \tag{10}$$

where $x_{\mathrm{c}}(k) \in \mathbb{R}^{n_{\mathrm{c}}}$. The feedback control (9)–(10) is described by $u(k) = G_{\mathrm{c}}(\mathbf{q}) y(k)$, where

$$G_{\mathrm{c}}(\mathbf{q}) = C_{\mathrm{c}}(\mathbf{q}I - A_{\mathrm{c}})^{-1} B_{\mathrm{c}}.$$

The closed-loop system with output feedback (9)–(10) is thus given by

$$\tilde{x}(k+1) = \tilde{A}\tilde{x}(k) + \tilde{D}_1 w(k), \tag{11}$$
$$y(k) = \tilde{C}\tilde{x}(k) + D_2 w(k), \tag{12}$$
$$z(k) = \tilde{E}_1 \tilde{x}(k), \tag{13}$$

where

$$\tilde{A} = \begin{bmatrix} A & BC_{\mathrm{c}} \\ B_{\mathrm{c}}C & A_{\mathrm{c}} \end{bmatrix}, \quad \tilde{D}_1 = \begin{bmatrix} D_1 \\ B_{\mathrm{c}} D_2 \end{bmatrix},$$
$$\tilde{C} = \begin{bmatrix} C & 0_{l_y \times n} \end{bmatrix}, \qquad \tilde{E}_1 = \begin{bmatrix} E_1 & E_2 C_{\mathrm{c}} \end{bmatrix}, \tag{14}$$

and

$$\tilde{x}(k) = \begin{bmatrix} x(k) \\ x_{\mathrm{c}}(k) \end{bmatrix} \in \mathbb{R}^{n+n_{\mathrm{c}}}. \tag{15}$$

The closed-loop system (11)–(13) is described by

$$\begin{bmatrix} z \\ y \end{bmatrix}^{\mathrm{T}} = \tilde{G}(z) w = \begin{bmatrix} \tilde{G}_{zw}(z) \\ \tilde{G}_{yw}(z) \end{bmatrix}^{\mathrm{T}} w,$$

where

$$\tilde{G}_{yw}(z) = \tilde{C}(zI - \tilde{A})^{-1} \tilde{D}_1 + D_2, \tag{16}$$
$$\tilde{G}_{zw}(z) = \tilde{E}_1(zI - \tilde{A})^{-1} \tilde{D}_1. \tag{17}$$

Furthermore, the characteristic polynomial of the closed-loop system is

$$\tilde{\mathcal{D}}(z) \triangleq \det(sI - \tilde{A}). \tag{18}$$

3 Linear-Quadratic-Gaussian Control

In this section, we discuss the closed-loop properties of the Linear-Quadratic-Gaussian (LQG) control. We first review the H_2 cost of the closed-loop system, and then, we derive the high-authority closed-loop pole locations from the return difference equation.

3.1 H_2 COST

Let $G_c \sim (A_c, B_c, C_c)$ denote an LTI controller such that $\tilde{A}$ is asymptotically stable. Then, the H_2 cost of the closed-loop system is given by

$$J(G_c) \stackrel{\triangle}{=} \|\tilde{G}\|_2, \tag{19}$$

where $\|.\|_2$ denotes the H_2 norm [20]. Furthermore,

$$J(G_c) = \lim_{k\to\infty} \mathbb{E}\left[z^{\mathrm{T}}(k)z(k)\right] = J_s(G_c) + J_c(G_c),$$

where

$$J_s(G_c) = \lim_{k\to\infty} \mathbb{E}\left[x^{\mathrm{T}}(k)R_1 x(k)\right],$$
$$J_c(G_c) = \lim_{k\to\infty} \mathbb{E}\left[u^{\mathrm{T}}(k)R_2 u(k)\right],$$

$J_s(G_c)$ is the state cost, $J_c(G_c)$ is the unnormalized control cost, $R_1 \stackrel{\triangle}{=} E_1^{\mathrm{T}}E_1$, and $R_2 \stackrel{\triangle}{=} E_2^{\mathrm{T}}E_2$. For convenience, we assume $E_1^{\mathrm{T}}E_2 = 0$.

Now, consider the discrete-time Lyapunov equation

$$Q = \tilde{A}Q\tilde{A}^{\mathrm{T}} + \tilde{D}_1\tilde{D}_1^{\mathrm{T}}. \tag{20}$$

Fact 3.1. Let $\tilde{Q} = \begin{bmatrix} Q_1 & Q_{12} \\ Q_{21} & Q_2 \end{bmatrix}$ satisfy the Lyapunov equation (20). Then,

$$J_s(G_c) = \mathrm{tr}(Q_1 R_1), \tag{21}$$
$$J_c(G_c) = \mathrm{tr}(Q_2 C_c^{\mathrm{T}} R_2 C_c). \tag{22}$$

The H_2 cost (19) of an arbitrary stabilizing LTI controller of arbitrary order can be evaluated using Fact 3.1. In particular, the LQG controller is the n^{th}-order optimal output feedback controller (9), (10) that minimizes (19) [20].

3.2 Closed-Loop Pole Locations

The LQG control problem is typically solved by combining the solutions to the Linear Quadratic Regulator (LQR) and the Linear Quadratic Estimator (LQE). The closed-loop system has $2n$ poles, n of which depends on the LQR design, and the remaining n poles depend on the LQE solution. This condition is known as *separation principle* [21, 22].

Consider the plant (1) with $D_1 = 0$. LQR controller is the state-feedback controller $u(k) = Kx(k)$ that minimizes (19), thus, in (2), $C = I_n$, and $D_2 = 0$. The closed-loop characteristic equation with LQR satisfies the following Lemma [22].

Lemma 3.1. Let $\mathcal{D}(z)$ and $\tilde{\mathcal{D}}(z)$ be defined as in (8), (18), $R_1 = E_1^{\mathrm{T}}E_1$, $R_2 = E_2^{\mathrm{T}}E_2$, and $E_1^{\mathrm{T}}E_2 = 0$. Then

$$\alpha\tilde{\mathcal{D}}(z^{-1})\tilde{\mathcal{D}}(z) = \mathcal{D}(z^{-1})\mathcal{D}(z) \cdot \det\left[R_2 + B^{\mathrm{T}}(z^{-1}I - A^{\mathrm{T}})^{-1}E_1^{\mathrm{T}}E_1(zI - A)^{-1}B\right], \tag{23}$$

where α is a positive real constant.

We now apply Lemma 3.1 to obtain the high-authority (that is, $R_2 = 0$) LQR closed-loop pole locations. Consider $G_{zu}(z) = H_d\frac{\mathcal{N}(z)}{\mathcal{D}(z)}$, where $\mathcal{D}(z)$ is a monic polynomial of degree n, $\mathcal{N}(z)$ is a monic polynomial of degree $n-d$, where $d \geq 1$ since $E_2 = 0$. Note that any common roots of $\mathcal{N}(z)$ and $\mathcal{D}(z)$ must lie inside the unit circle since (A, B) is stabilizable and (A, E_1) is detectable. Now, consider the polynomial factorization

$$\mathcal{N}(z) = \beta_S(z)\beta_U(z), \tag{24}$$

where $\beta_U(z)$ and $\beta_S(z)$ are monic polynomials of degree n_U and $n_S = n - d - n_U$ respectively, and each NMP zero of $G_{zu}(z)$ is a root of $\beta_U(z)$. Furthermore, let

$$\bar{\beta}_U(z) \stackrel{\triangle}{=} \beta_U(z^{-1}) \tag{25}$$

be the monic polynomial of order n_U such that the reciprocal of each zero of $\beta_U(z)$ is a root of $\bar{\beta}_U(z)$. For example, for $\beta_U(\mathbf{q}) = (\mathbf{q}-1.2)^2(\mathbf{q}-0.8-\mathrm{j}0.9)(\mathbf{q}-0.8+\mathrm{j}0.9)$, we have

$$\bar{\beta}_U(\mathbf{q}) = \left(\mathbf{q} - \frac{1}{1.2}\right)^2\left(\mathbf{q} - \frac{1}{0.8+\mathrm{j}0.9}\right)\left(\mathbf{q} - \frac{1}{0.8-\mathrm{j}0.9}\right).$$

Proposition 3.1. Let $l_u = 1$, $l_z = 1$. Then, in the high-authority LQR control with $R_2 = 0$, the closed-loop poles are the roots of

$$\tilde{\mathcal{D}}(z) = z^d\beta_S(z)\bar{\beta}_U(z). \tag{26}$$

Proof 3.1. Since $R_2 = 0$, we have $E_2 = 0$, and, it follows

from (5), (23), (24) that

$$\alpha\tilde{\mathcal{D}}(z^{-1})\tilde{\mathcal{D}}(z) = H_d^2\mathcal{D}(z^{-1})\mathcal{D}(z)\frac{\beta_S(z^{-1})\bar{\beta}_U(z)}{\mathcal{D}(z^{-1})}\frac{\beta_S(z)\beta_U(z)}{\mathcal{D}(z)},$$
$$= H_d^2\beta_S(z^{-1})\bar{\beta}_U(z)\beta_S(z)\beta_U(z). \quad (27)$$

The optimal closed-loop system must be stable since the open-loop plant is stabilizable and detectable, hence, the unstable roots of (27) cannot the poles of $\tilde{\mathcal{D}}(z)$. Thus, $n-d$ poles of $\tilde{\mathcal{D}}(z)$ are the roots of $\beta_S(z)\bar{\beta}_U(z)$. The remaining d poles of $\tilde{\mathcal{D}}(z)$ must be given by z^d since otherwise (23) would not hold. □

Proposition 3.1 shows that in discrete-time LQR, we obtain a similar result to the continuous-time case: β_S closed-loop poles approach the MP zeros, β_U poles approach the reciprocals of the NMP zeros, and the remaining poles approach zero, as R_2 approaches zero. Unlike the continuous-time case, the pole locations are symmetric with respect to the unit circle rather than the imaginary axis, as expected from the return difference equation (23).

We now give the dual of the Proposition 3.1 for the closed-loop poles assigned by the LQE without proof, which, together with Proposition 3.1, provides the closed-loop pole locations assigned by the high-authority discrete-time LQG compensator under no measurement noise, that is, $D_2 = 0$. Consider $G_{yw}(z) = H_{yw,d_{yw}}\frac{\mathcal{N}_{yw}(z)}{\mathcal{D}(z)}$, where $\mathcal{N}_{yw}(z)$ is a monic polynomial of degree $n-d_{yw}$, where $d_{yw} \geq 1$ since $D_2 = 0$. Note that any common roots of $\mathcal{N}_{yw}(z)$ and $\mathcal{D}(z)$ must lie inside the unit circle since (A, D_1) is stabilizable and (A, C) is detectable. Now, consider the polynomial factorization

$$\mathcal{N}_{yw}(z) = \beta_{yw,S}(z)\beta_{yw,U}(z), \quad (28)$$

where $\beta_{yw,U}(z)$ and $\beta_{yw,S}(z)$ are monic polynomials of degree $n_{yw,U}$ and $n_{yw,S} = n - d_{yw} - n_{yw,U}$ respectively, and each NMP zero of $G_{yw}(z)$ is a root of $\beta_{yw,U}(z)$. Let $\bar{\beta}_{yw,U}(z) \triangleq \beta_{yw,U}(z^{-1})$ be the monic polynomial of order $n_{yw,U}$ such that the reciprocal of each zero of $\beta_{yw,U}(z)$ is a root of $\bar{\beta}_{yw,U}(z)$.

Proposition 3.2. Let $l_u = 1$, $l_w = 1$, $D_1 \neq 0$, $D_2 = 0$, and $\sigma_w^2 > 0$. Let $u(k) = K\hat{x}(k)$, where $\hat{x}$ is the state estimate obtained with the LQE. The closed-loop system has $2n$ closed-loop poles, n of which are the roots of

$$z^{d_{yw}}\beta_{yw,S}(z)\bar{\beta}_{yw,U}(z) \quad (29)$$

Therefore, the closed-loop poles with the LQG compensator has $2n$ poles, and, in high-authority with no measurement noise, n_S poles are at the MP zeros of $G_{zu}(z)$, $n_{yw,U}$ poles are at the MP zeros of $G_{yw}(z)$, n_U poles are at the reciprocals of the NMP zeros of $G_{zu}(z)$, $n_{yw,U}$ poles are at the reciprocals of the NMP zeros of $G_{yw}(z)$, and the remaining $d + d_{yw}$ poles are at zero.

4 RETROSPECTIVE COST ADAPTIVE CONTROL

4.1 Broadband Disturbance Rejection with RCAC

Retrospective cost adaptive control (RCAC) is a direct, digital adaptive output feedback algorithm applicable to MIMO, possibly nonminimum-phase and unstable plants. For the adaptive system, the matrices $A_c = A_c(k)$, $B_c = B_c(k)$, and $C_c = C_c(k)$ in (9), (10) may be time varying, and thus the transfer function models (16), (17) may not be valid during controller adaptation. However, (11)–(13) illustrates the structure of the time-varying closed-loop system in which $\tilde{A} = \tilde{A}(k)$, $\tilde{D}_1 = \tilde{D}_1(k)$ and $\tilde{E}_1 = \tilde{E}_1(k)$.

The goal is to determine the ability of the asymptotic RCAC controller $G_{c,\infty}$ to minimize $J(G_c)$ in the presence of the disturbance w with limited modeling information about the plant and the noise covariances. RCAC requires a measurement of $z(k)$ for controller update. The block diagram of the adaptive feedback system is shown in Figure 1.

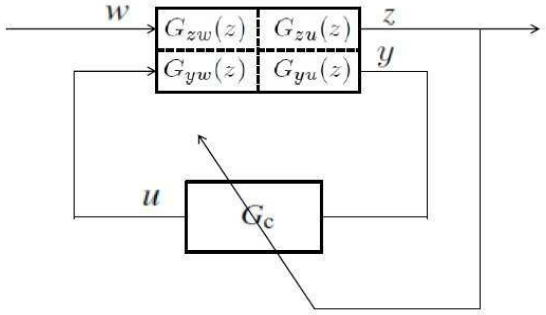

Figure 1. RCAC FEEDBACK SYSTEM.

To compare RCAC performance to the optimal LQG performance with noise-free measurements, we create a Pareto tradeoff curve involving J_s and the normalized control cost $\hat{J}_c \triangleq J_c/R_2$ by computing LQG controllers for a range of values of R_2. Next, to assess the asymptotic performance of RCAC, we simulate RCAC with a white disturbance signal. After convergence, we evaluate $J_s(G_{c,\infty})$ and $\hat{J}_c(G_{c,\infty})$, where $G_{c,\infty} \sim (A_{c,\infty}, B_{c,\infty}, C_{c,\infty})$ is a realization of the asymptotic controller. Finally, we compare the asymptotic H_2 cost with the LQG Pareto tradeoff curve.

4.2 Control Law

We represent Eqs. (9), (10) by

$$u(k) = \theta^{\mathrm{T}}(k)\phi(k-1), \quad (30)$$

where

$$\theta(k) = \left[N_1^{\mathrm{T}}(k) \ \cdots \ N_{n_c}^{\mathrm{T}}(k) \ M_1^{\mathrm{T}}(k) \ \cdots \ M_{n_c}^{\mathrm{T}}(k)\right]^{\mathrm{T}}, \tag{31}$$

$$\phi(k-1) = \left[y^{\mathrm{T}}(k-1) \ \cdots \ y^{\mathrm{T}}(k-n_c) \ u^{\mathrm{T}}(k-1) \ \cdots \ u^{\mathrm{T}}(k-n_c)\right]^{\mathrm{T}}, \tag{32}$$

and, for all $1 \le i \le n_c$, $N_i(k) \in \mathbb{R}^{l_y \times l_u}$, $M_i(k) \in \mathbb{R}^{l_u \times l_u}$. The control law (30) can be reformulated as

$$u(k) = \Phi(k-1)\Theta(k), \tag{33}$$

where

$$\Phi(k-1) \triangleq I_{l_u} \otimes \phi^{\mathrm{T}}(k-1) \in \mathbb{R}^{l_u \times l_u n_c (l_u+l_y)}, \tag{34}$$

$$\Theta(k) \triangleq \mathrm{vec}(\theta(k)) \in \mathbb{R}^{l_u n_c (l_u+l_y)}, \tag{35}$$

"$\otimes$" denotes the Kronecker product, and "vec" is the column-stacking operator.

4.3 Retrospective Performance

For a positive integer n_f, we define

$$G_f(\mathbf{q}) \triangleq D_f^{-1}(\mathbf{q}) N_f(\mathbf{q}) \in \mathbb{R}^{l_z \times l_u}[\mathbf{q}], \tag{36}$$

where

$$\begin{aligned} N_f(\mathbf{q}) &\triangleq K_1 \mathbf{q}^{n_f-1} + K_2 \mathbf{q}^{n_f-2} + \cdots + K_{n_f}, \\ D_f(\mathbf{q}) &\triangleq I_{l_z} \mathbf{q}^{n_f} + A_1 \mathbf{q}^{n_f-1} + A_2 \mathbf{q}^{n_f-2} + \cdots + A_{n_f}, \end{aligned} \tag{37}$$

$K_i \in \mathbb{R}^{l_z \times l_u}$ for $1 \le i \le r$, $A_j \in \mathbb{R}^{l_z \times l_z}$ for $1 \le j \le r$, $n_f \ge 1$ is the order of G_f, and each polynomial entry of $D_f(\mathbf{q})$ is asymptotically stable. Next, for $k \ge 1$, we define the *retrospective performance variable*

$$\hat{z}(\hat{\Theta}(k),k) \triangleq z(k) + \Phi_f(k-1)\hat{\Theta}(k) - u_f(k), \tag{38}$$

with

$$\Phi_f(k-1) \triangleq G_f(\mathbf{q})\Phi(k-1) \in \mathbb{R}^{l_z \times l_u n_c (l_u+l_y)}, \tag{39}$$

$$u_f(k) \triangleq G_f(\mathbf{q})u(k) \in \mathbb{R}^{l_z}, \tag{40}$$

where $\hat{\Theta}(k)$ is determined by optimization below.

If G_f is chosen as a finite-impulse-response (FIR) filter with $K_i = H_i$, $A_i = 0$ for all $i \in \{1,\ldots,n_f\}$, then $\hat{z}(\hat{\Theta}(k),k)$ represents the performance that would have been obtained if the controller $\hat{\Theta}(k)$ had been used in the past n_f steps. In this case, minimizing $\hat{z}^{\mathrm{T}}(\hat{\Theta}(k),k)\hat{z}(\hat{\Theta}(k),k)$ provides the retrospectively optimized controller $\hat{\Theta}(k)$ for the past n_f steps. However, G_f need not be constructed using Markov parameters, and, infinite-impulse-response (IIR) construction of G_f provides greater flexibility in the assignment of asymptotic closed-loop pole locations, as discussed in Section 5.

4.4 Cumulative Cost and Update Law

For $k > 0$, we define the cumulative cost function

$$\begin{aligned} J(\hat{\Theta}(k),k) \triangleq{}& \sum_{i=1}^{k} \lambda^{k-i} \hat{z}^{\mathrm{T}}(\hat{\Theta}(k),i)\hat{z}(\hat{\Theta}(k),i) \\ &+ \sum_{i=1}^{k} \lambda^{k-i} \eta(i) \hat{\Theta}^{\mathrm{T}}(k) \Phi_f^{\mathrm{T}}(i-1)\Phi_f(i-1)\hat{\Theta}(k) \\ &+ \lambda^k (\hat{\Theta}(k)-\Theta_0)^{\mathrm{T}} P_0^{-1} (\hat{\Theta}(k)-\Theta_0), \end{aligned} \tag{41}$$

where $\lambda \in (0,1]$, $P_0 \in \mathbb{R}^{l_u n_c (l_u+l_y) \times l_u n_c (l_u+l_y)}$ is positive definite, $\eta(k) \ge 0$, and $\Theta_0 \in \mathbb{R}^{l_u n_c (l_u+l_y)}$. In this paper, we choose

$$\eta(k) \triangleq \eta_0 \sum_{j=0}^{p_c-1} z^{\mathrm{T}}(k-j) z(k-j). \tag{42}$$

where $\eta_0 \ge 0$, and $p_c \ge 1$. Note that $\eta(k)$ is a performance-dependent weighting which increases as the magnitude of z increases.

The following result provides the global minimizer of the cost function (41).

Proposition 4.1. Let $P(0) = P_0$ and $\Theta(0) = \Theta_0$. Then, for all $k \ge 1$, the cumulative cost function (41) has a unique global minimizer $\Theta(k)$ given by

$$\Theta(k) = \Theta(k-1) - \frac{1}{1+\eta(k)} P(k-1)\Phi_f^{\mathrm{T}}(k-1)\Lambda^{-1}(k)\varepsilon(k), \tag{43}$$

where

$$\begin{aligned} \Lambda(k) &\triangleq \frac{\lambda}{1+\eta(k)} I_{l_z} + \Phi_f(k-1)P(k-1)\Phi_f^{\mathrm{T}}(k-1), \\ \varepsilon(k) &\triangleq z(k) - u_f(k) + (1+\eta(k))\hat{u}_f(k), \\ \hat{u}_f(k) &\triangleq \Phi_f(k-1)\Theta(k-1), \end{aligned}$$

and $P(k)$ satisfies

$$P(k) = \frac{1}{\lambda}[P(k-1) - P(k-1)\Phi_{\mathrm{f}}^{\mathrm{T}}(k-1)\Lambda^{-1}(k)\Phi_{\mathrm{f}}(k-1)P(k-1)]. \quad (44)$$

Proof 4.1. The result follows from RLS theory [3, 4].

5 CONTROLLER CONSTRUCTION

In this section, we discuss the construction of G_{f} for SISO plants. Extensions to MIMO plants are given in [16].

We first discuss the NMP-zero-based construction of the numerator polynomial $N_{\mathrm{f}}(\mathbf{q})$ of G_{f}. This construction requires knowledge of the NMP-zeros of G_{zu}, if any. Alternative methods for plants with unknown NMP zeros are presented in [19], which use the performance-dependent weighting $\eta(k)$ to prevent unstable pole-zero cancellation. Next, we discuss the construction of $D_{\mathrm{f}}(\mathbf{q})$ for the assigning target closed-loop poles.

5.1 NMP-Zero-Based Construction of N_{f}

We rewrite (1), (3) as $G_{zu}(\mathbf{q}) = H_d \frac{\mathcal{N}(\mathbf{q})}{\mathcal{D}(\mathbf{q})}$ and the polynomial factorization (24). Assume that H_d and the nonminimum-phase (NMP) zeros of G_{zu}, if any, are known. The NMP-zero-based construction of N_{f} is given by

$$N_{\mathrm{f}}(\mathbf{q}) = H_d \mathbf{q}^{n_{\mathrm{f}}-n_{\mathrm{U}}-d}\beta_{\mathrm{U}}(\mathbf{q}), \quad (45)$$

where the choice of n_{f} is explained below in Section 5.2. If G_{zu} is minimum-phase, then $\beta_{\mathrm{U}}(\mathbf{q}) = 1$, and thus $N_{\mathrm{f}}(\mathbf{q}) = H_d \mathbf{q}^{n_{\mathrm{f}}-n_{\mathrm{U}}-d}$.

Note that this construction requires the knowledge of the first nonzero Markov parameter H_d of G_{zu}, the relative degree d of G_{zu}, and the NMP zeros of G_{zu}.

5.2 Construction of D_{f} for Recovering High-Authority LQG Performance

It is shown in [17] that RCAC is able to drive the closed-loop dynamics to an arbitrary location determined by the roots of the asymptotically stable monic polynomial $D_{\mathrm{f}}(\mathbf{q})$. In particular, n_{S} closed-loop poles cancel the MP zeros of G_{zu}, that is, the open-loop zeros that are not zeros of $N_{\mathrm{f}}(\mathbf{q})$. Furthermore, n_{f} closed-loop poles are driven near the roots of D_{f}, and the remaining closed-loop poles are asymptotically driven to zero. In this section, we present a method for exploiting this property so that RCAC can mimic the response of the high-authority LQG controller with no measurement noise.

Consider the n^{th}-order plant (1)–(3) with the $n_{\mathrm{c}}^{\mathrm{th}}$-order output feedback controller (33)–(35). For consistency with the LQG controller, we let $n_{\mathrm{c}} = n$, and thus the closed-loop system is of order $2n$. Furthermore, we assume that the performance variable $z(k)$ is the input to the controller so that $y = z$, and the input signal coincides with the disturbance signal, hence $B = D_1$, and thus $G_{zu} = G_{yw}$. Therefore, with $R_1 = E_1^{\mathrm{T}}E_1$, $R_2 = 0$, LQG control places two poles at each open-loop MP zero of G_{zu}, two poles at the reciprocal of each open-loop NMP zero of G_{zu}, and it places the remaining closed-loop poles (that is, $2(n - n_{\mathrm{S}} - n_{\mathrm{U}}) = 2d$ poles) at zero, as discussed in Section 3.2. In order for RCAC to recover the high-authority LQG performance, we let

$$D_{\mathrm{f}}(\mathbf{q}) = \beta_{\mathrm{S}}(\mathbf{q})\bar{\beta}_{\mathrm{U}}^2(\mathbf{q}), \quad (46)$$

where $\bar{\beta}_{\mathrm{U}}$ is as defined in (25). Hence, the order n_{f} of D_{f} is $n_{\mathrm{f}} = n_{\mathrm{S}} + 2n_{\mathrm{U}}$. Note that since RCAC cancels the MP zeros of G_{zu}, D_{f} needs to have only one root at each MP zero of G_{zu} in order to have two closed-loop poles at each minimum-phase zero. However, D_{f} has two poles at the reciprocal at each NMP zero of G_{zu} since RCAC does not place the closed-loop poles at the reciprocals of the open-loop NMP zeros.

Example 5.1. Consider

$$G_{zu}(\mathbf{q}) = -2\frac{(\mathbf{q}-1.1)(\mathbf{q}-0.4)}{(\mathbf{q}-1.3)(\mathbf{q}-0.5-\mathrm{j}0.5)(\mathbf{q}-0.5+\mathrm{j}0.5)}.$$

To assign the target closed-loop poles at the high-authority LQG locations, we let

$$D_{\mathrm{f}}(\mathbf{q}) = (\mathbf{q}-0.4)\left(\mathbf{q}-\frac{1}{1.1}\right)^2,$$

so that $n_{\mathrm{f}} = 3$. Thus, it follows from (45) that

$$N_{\mathrm{f}}(\mathbf{q}) = -2\mathbf{q}(\mathbf{q}-1.1).$$

6 Numerical Examples

We now illustrate broadband noise rejection with RCAC and compare the performance of the asymptotic controller to LQG. We first consider the case where the only available modeling information for RCAC is the relative degree d and the first nonzero Markov parameter H_d of the plant G_{zu}. Next, we consider the case where d, H_d, and the plant zeros are known. In this case, we choose D_{f} to assign the target closed-loop poles to high-authority LQG pole locations as discussed in the previous section.

We consider only SISO plants, therefore, $l_u = l_y = 1$. In all examples, the plant is scaled so that $H_d = 1$. Furthermore, the unknown standard deviation of the gaussian disturbance σ_w is normalized to 1 in all simulations, and, in each example, we set the initial condition $x(0)$ to be a randon vector with $\|x(0)\| = 5000$. In all cases, we let $B = D_1$, and $y = z$, thus $G_{zw} = G_{zu} = G_{yw} = G_{yu}$. This assumption is not required for RCAC, but it makes the assignment of the target closed-loop

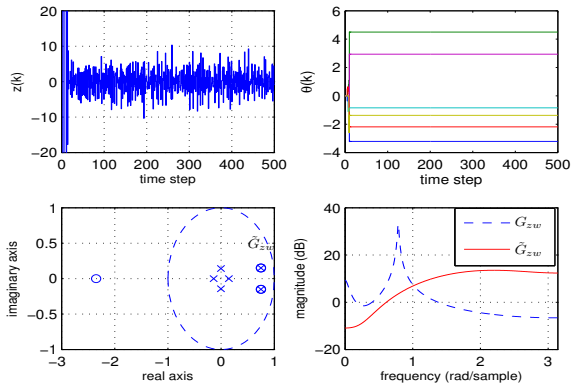

Figure 2. EXAMPLE 6.1: MINIMUM-PHASE, ASYMPTOTICALLY STABLE PLANT. RCAC SUPPRESSES THE OPEN-LOOP LIGHTLY DAMPED MODE, AND THE PERFORMANCE REACHES ITS STEADY-STATE LEVEL IN ABOUT 9 STEPS. THE RMS VALUE OF THE CLOSED-LOOP BODE GAIN IS 10.9 DB. RCAC CANCELS THE OPEN-LOOP ZEROS, AND PLACES THE REMAINING POLES NEAR THE ORIGIN. THE CLOSED-LOOP POLES ARE NOT DRIVEN NEAR THE ASYMPTOTIC, HIGH-AUTHORITY LQG POLE LOCATIONS.

poles more convenient since the high-authority symmetric root-locus depends on only the zeros of G_{zu} in this case. Furthermore, in all examples, we assume that the measurement of z is noise-free. Finally, in each example, we show the time traces of the performance variable $z(k)$ and the controller gain vector $\theta(k)$, as well as time-domain and frequency-domain characteristics of the closed-loop system after convergence.

6.1 Numerical Examples for Plants with Unknown Zeros

In this section, we consider broadband noise rejection for plants with unknown zeros. Since the zeros are unknown, we set $G_{\mathrm{f}}(q) = \frac{H_d}{\mathbf{q}^d}$ in all examples. Furthermore, if the plant is NMP, we let $\eta_0 > 0$ to prevent unstable pole-zero cancellation.

Example 6.1. [Minimum-phase, asymptotically stable plant.] Consider G_{zu} with stable poles $0.7 + \mathrm{j}0.7$, $0.7 - \mathrm{j}0.7$, 0.95, and minimum-phase zeros $0.75 \pm \mathrm{j}0.15$. We choose the RCAC tuning parameters $P_0 = I_{2n}$ and $\eta_0 = 0$. We first simulate the open-loop system for 5 time steps, and then turn RCAC on at $k = 5$. The closed-loop response is shown in Figure 2. ■

Example 6.2. [Minimum-phase, unstable plant.] Consider G_{zu} with stable poles $0.8 \pm \mathrm{j}0.5$, unstable pole 1.25, and minimum-phase zeros 0.4 and 0.85. We choose $P_0 = I_{2n}$ and $\eta_0 = 0$. We first simulate the open-loop system for 5 time steps, and turn RCAC on at $k = 5$. The closed-loop response is shown in Figure 3. ■

Example 6.3. [Nonminimum-phase, asymptotically stable plant.] Consider G_{zu} with stable poles 0.99, $0.6 \pm \mathrm{j}0.75$, and unknown nonminimum-phase zeros 1.4 and 2. We choose $P_0 = I_{2n}$,

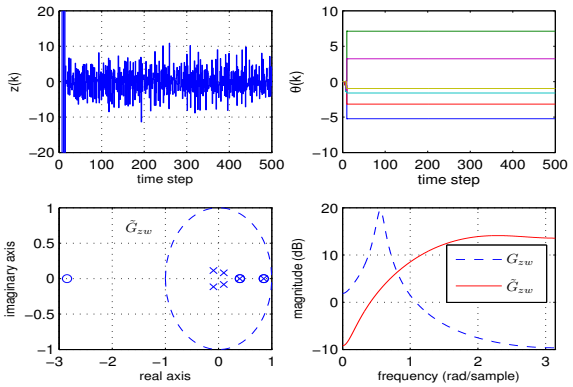

Figure 3. EXAMPLE 6.2: MINIMUM-PHASE, UNSTABLE PLANT. RCAC IS TURNED ON AT $k = 5$, AND THE PERFORMANCE REACHES ITS STEADY-STATE LEVEL IN ABOUT 9 STEPS. THE RMS VALUE OF THE CLOSED-LOOP BODE GAIN IS 11.7 DB. RCAC STABILIZES THE CLOSED-LOOP SYSTEM, CANCELS THE OPEN-LOOP ZEROS, AND PLACES THE REMAINING POLES NEAR ZERO. THE CLOSED-LOOP POLES ARE NOT DRIVEN NEAR THE HIGH-AUTHORITY LQG POLE LOCATIONS.

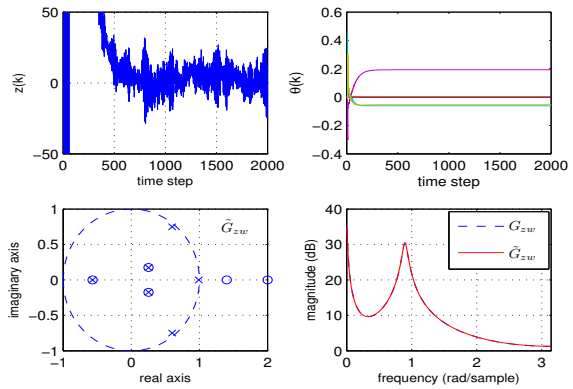

Figure 4. EXAMPLE 6.3: NONMINIMUM-PHASE, ASYMPTOTICALLY STABLE PLANT. THE RMS VALUE OF THE CLOSED-LOOP BODE GAIN IS 17.9 DB. RCAC DOES NOT CHANGE THE LOCATION OF THE OPEN-LOOP POLES, AND THE FREQUENCY DOMAIN CHARACTERISTICS OF THE OPEN-LOOP AND CLOSED-LOOP SYSTEMS ARE SIMILAR. THE CLOSED-LOOP POLES ARE NOT DRIVEN NEAR THE ASYMPTOTIC, HIGH-AUTHORITY LQG POLE LOCATIONS.

and, to prevent unstable pole-zero cancellation due to the unknown NMP-zeros, we choose $\eta_0 = 0.1$. We first simulate the open-loop system for 5 time steps, and then turn RCAC on at $k = 5$. The closed-loop response is shown in Figure 4. ■

6.2 Numerical Examples for Plants with Known Zeros

In this section, we consider broadband noise rejection for plants with known zeros. Since the zeros of the plant are known, we construct G_{f} as outlined in Section 5 to asymptotically recover the high-authority LQG performance.

Example 6.4. [Minimum-phase, stable plant.] Consider the same plant $G_{zu}(z)$ of Example 6.1. Assuming the zeros of

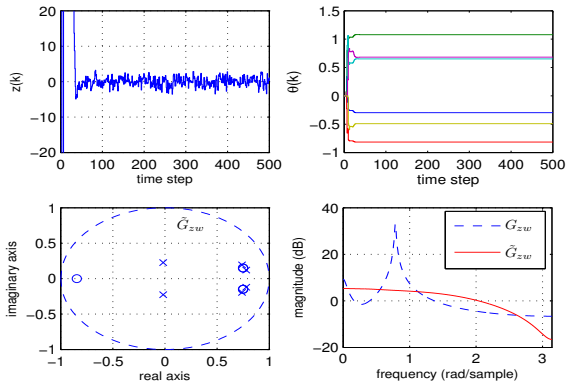

Figure 5. EXAMPLE 6.4: MINIMUM-PHASE, ASYMPTOTICALLY STABLE PLANT, RCAC IS TURNED ON AT $k = 5$ WITH THE HIGH-AUTHORITY LQG POLE LOCATIONS SET AS THE TARGET CLOSED-LOOP DYNAMICS. RCAC SUPPRESSES THE OPEN-LOOP LIGHTLY-DAMPED MODE, AND THE PERFORMANCE REACHES ITS STEADY-STATE LEVEL IN ABOUT 30 STEPS. THE RMS VALUE OF THE BODE GAIN IS 2.4 DB, HENCE, 8.5 DB MORE SUPPRESSION IS OBTAINED COMPARED TO FIG. 2. RCAC PLACES TWO POLES NEAR EACH OPEN-LOOP ZERO, AND PLACES THE REMAINING POLES NEAR THE ORIGIN. THEREFORE, THE CLOSED-LOOP POLES ARE DRIVEN NEAR THE HIGH-AUTHORITY LQG POLE LOCATIONS.

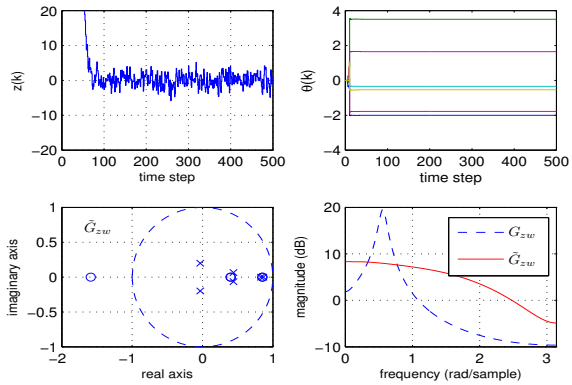

Figure 6. EXAMPLE 6.5: MINIMUM-PHASE, UNSTABLE PLANT, RCAC IS TURNED ON AT $k = 5$ WITH THE HIGH-AUTHORITY LQG POLE LOCATIONS SET AS THE TARGET CLOSED-LOOP DYNAMICS. RCAC STABILIZES THE CLOSED-LOOP SYSTEM, AND THE PERFORMANCE REACHES ITS STEADY-STATE LEVEL IN ABOUT 55 STEPS. THE RMS VALUE OF THE BODE GAIN IS 5.5 DB, HENCE, 6.2 DB MORE SUPPRESSION IS OBTAINED COMPARED TO FIG. 3. RCAC PLACES TWO POLES NEAR EACH OPEN-LOOP ZERO, AND PLACES THE REMAINING POLES NEAR THE ORIGIN. THEREFORE, THE CLOSED-LOOP POLES ARE DRIVEN NEAR THE ASYMPTOTIC, HIGH-AUTHORITY LQG POLE LOCATIONS.

G_{zu} are known, we let $N_\mathrm{f} = H_1\mathbf{q}$ and $D_\mathrm{f} = \beta_\mathrm{S}(\mathbf{q}) = (\mathbf{q} - 0.75 - \mathrm{j}0.15)(\mathbf{q} - 0.75 + \mathrm{j}0.15)$. Therefore, the target closed-loop dynamics are the high-authority LQG pole locations, that is, two poles at each open-loop zero location, and two poles at the origin. We choose $P_0 = I_{2n}$, and $\eta_0 = 0$. We first simulate the open-loop system for 5 time steps, and then turn RCAC on at $k = 5$. The closed-loop response is shown in Figure 5. ■

Example 6.5. [Minimum-phase, unstable plant.] Consider the same plant G_{zu} of Example 6.2. Assuming the zeros of G_{zu} are known, we let $N_\mathrm{f} = H_1\mathbf{q}$ and $D_\mathrm{f} = \beta_\mathrm{S}(\mathbf{q}) = (\mathbf{q} - 0.85)(\mathbf{q} - 0.4)$. Therefore, the target closed-loop dynamics are the high-authority LQG pole locations, that is, two poles at each open-loop zero location, and two poles at the origin. We choose $P_0 = I_{2n}$, and $\eta_0 = 0$. We first simulate the open-loop system for 5 time steps, and then turn RCAC on at $k = 5$. The closed-loop response is shown in Figure 6. ■

Example 6.6. [Nonminimum-phase, stable plant.] Consider the same plant G_{zu} of Example 6.3. Assuming the zeros of G_{zu} are known, we assign the target closed-loop dynamics to the reciprocals of the open-loop NMP zeros by letting $D_\mathrm{f} = \tilde{\beta}_\mathrm{U}^2(\mathbf{q}) = (\mathbf{q} - \frac{1}{2})^2(\mathbf{q} - \frac{1}{1.4})^2$, and we choose $N_\mathrm{f} = H_1\mathbf{q}\beta_\mathrm{U}(\mathbf{q}) = \mathbf{q}(\mathbf{q} - 2)(\mathbf{q} - 1.4)$. We choose $P_0 = I_{2n}$, and $\eta_0 = 0$. We first simulate the open-loop system for 5 steps, and then turn RCAC on at $k = 5$. The closed-loop response is shown in Figure 7. ■

Example 6.7. [Nonminimum-phase, unstable plant.] Consider G_{zu} with stable poles $0.3 \pm \mathrm{j}0.85$, unstable pole 1.3, and nonminimum-phase zeros $1.1 \pm \mathrm{j}0.8$. We first do not assign target closed-loop dynamics and choose $D_\mathrm{f}(\mathbf{q}) = \mathbf{q}^3$, $N_\mathrm{f} = H_1\beta_\mathrm{U}(\mathbf{q}) = (\mathbf{q} - 1.1 - \mathrm{j}0.8)(\mathbf{q} - 1.1 + \mathrm{j}0.8)$. We let $P_0 = I_{2n}$, and $\eta_0 = 0$. We simulate the open-loop system for 5 steps, and then turn RCAC on at $k = 5$. The closed-loop response is shown in Figure 8.

Now, we assign the target closed-loop dynamics to the reciprocals of the open-loop NMP zeros by letting $D_\mathrm{f} = \tilde{\beta}_\mathrm{U}^2(\mathbf{q}) = (\mathbf{q} - \frac{1}{1.1+\mathrm{j}0.8})^2(\mathbf{q} - \frac{1}{1.1-\mathrm{j}0.8})^2$, and we choose $N_\mathrm{f} = H_1\mathbf{q}\beta_\mathrm{U}(\mathbf{q}) = \mathbf{q}(\mathbf{q} - 1.1 - \mathrm{j}0.8)(\mathbf{q} - 1.1 + \mathrm{j}0.8)$. We choose $P_0 = I_{2n}$ and $\eta_0 = 0$. We simulate the open-loop system for 5 steps, and then turn RCAC on at $k = 5$. The closed-loop response is shown in Figure 9. ■

6.3 State Cost and Control Cost with RCAC

We now investigate the asymptotic performance of RCAC in the numerical examples considered in Sections 6.1 and 6.2. In particular, to assess the performance of RCAC, we compute the state cost $J_s(G_\mathrm{c})$ and the normalized control cost $\hat{J}_c(G_\mathrm{c})$ for the asymptotic closed-loop system using the equations given in Fact 3.1.

First, we investigate the performance of RCAC without and with the target closed-loop dynamics assigned at LQG locations. Figure 10 illustrates the performance of RCAC with MP asymptotically stable, MP unstable, NMP asymptotically stable, and NMP unstable plants considered in the previous sections. In all cases, assigning the closed-loop poles to the asymptotic high-authority LQG locations substantially decreases the asymptotic state cost of the closed-loop system, and in most cases, it also provides reduced control effort, except for the NMP stable case.

We now compare the H_2 performance of the asymptotic RCAC controller under limited modeling information with the

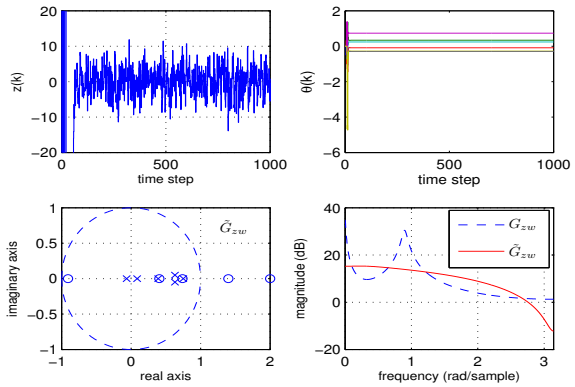

Figure 7. Example 6.6: NONMINIMUM-PHASE, ASYMPTOTICALLY STABLE PLANT, RCAC IS TURNED ON AT $k = 5$ WITH TARGET CLOSED-LOOP DYNAMICS ASSIGNED TO THE HIGH-AUTHORITY LQG POLE LOCATIONS. RCAC SUPPRESSES THE OPEN-LOOP LIGHTLY-DAMPED MODE, AND THE PERFORMANCE REACHES ITS STEADY-STATE LEVEL IN ABOUT 60 STEPS. THE RMS VALUE OF THE CLOSED-LOOP BODE GAIN IS 11.9 DB, HENCE, 6 DB MORE SUPPRESSION IS OBTAINED COMPARED TO FIG. 4. RCAC PLACES TWO POLES NEAR THE RECIPROCALS OF EACH OPEN-LOOP NMP ZERO, AND PLACES THE REMAINING POLES NEAR THE ORIGIN. THEREFORE, THE CLOSED-LOOP POLES ARE DRIVEN NEAR THE HIGH-AUTHORITY LQG POLE LOCATIONS.

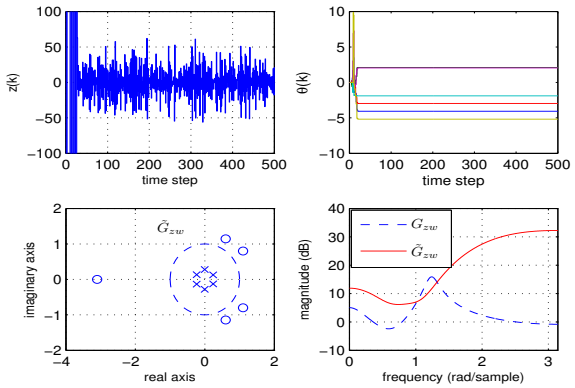

Figure 8. EXAMPLE 6.7: NONMINIMUM-PHASE, UNSTABLE PLANT, TARGET CLOSED-LOOP POLES ARE NOT ASSIGNED. RCAC STABILIZES THE CLOSED-LOOP SYSTEM, AND THE PERFORMANCE REACHES ITS STEADY-STATE LEVEL IN ABOUT 20 STEPS. THE RMS VALUE OF THE CLOSED-LOOP BODE PLOT IS 27.1 DB. SINCE N_{f} CONTAINS ALL THE ZEROS OF G_{zu}, RCAC PLACES ALL THE CLOSED-LOOP POLES NEAR THE ORIGIN. THEREFORE, THE CLOSED-LOOP POLES ARE NOT DRIVEN NEAR THE ASYMPTOTIC, HIGH-AUTHORITY LQG POLE LOCATIONS.

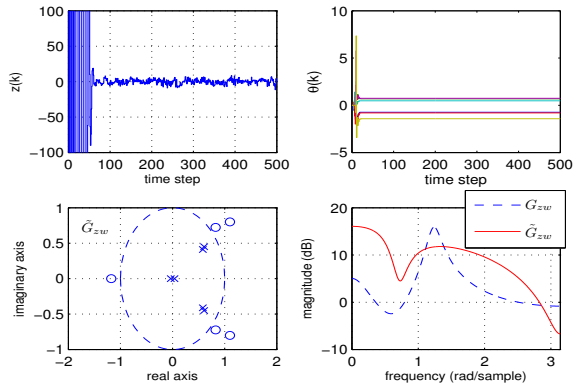

Figure 9. EXAMPLE 6.7: NONMINIMUM-PHASE, UNSTABLE PLANT, TARGET CLOSED-LOOP DYNAMICS ARE ASSIGNED TO THE HIGH-AUTHORITY LQG POLE LOCATIONS. RCAC STABILIZES THE CLOSED-LOOP SYSTEM, AND THE PERFORMANCE REACHES ITS STEADY-STATE LEVEL IN ABOUT 50 STEPS. THE RMS VALUE OF THE CLOSED-LOOP SYSTEM IS 10.8 DB, HENCE, 16.3 DB MORE SUPPRESSION IS OBTAINED COMPARED TO FIG. 8. RCAC PLACES TWO POLES NEAR THE RECIPROCALS OF EACH NMP ZERO, AND PLACES THE REMAINING POLES NEAR THE ORIGIN. THEREFORE, THE CLOSED-LOOP POLES ARE DRIVEN NEAR THE ASYMPTOTIC, HIGH-AUTHORITY LQG POLE LOCATIONS.

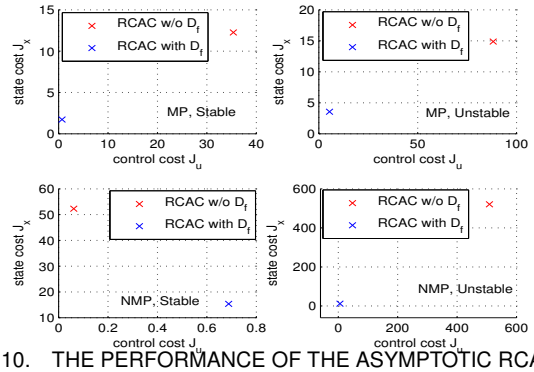

Figure 10. THE PERFORMANCE OF THE ASYMPTOTIC RCAC CONTROLLER FOR THE NUMERICAL EXAMPLES OF SECTIONS 6.1 AND 6.2. IN ALL CASES, THE STATE COST IS SMALLEST WHEN D_{f} IS CONSTRUCTED AS IN SECTION 5.2 FOR ALLOWING RCAC TO MIMIC LQG. FURTHERMORE, IN MOST CASES, THIS ALSO LEADS TO SMALLER CONTROL EFFORT. THEREFORE, RCAC IS MORE EFFECTIVE WHEN D_{f} IS CONSTRUCTED TO ASSIGN THE TARGET CLOSED-LOOP DYNAMICS TO THE ASYMPTOTIC HIGH-AUTHORITY LQG LOCATIONS.

performance of LQG under complete modeling information. In particular, we focus on the performance of RCAC with D_{f} constructed as in Section 5.2, where the required modeling information is the first nonzero Markov parameter, the relative degree, and the location of the open-loop zeros. Figure 11 illustrates the optimal LQG curve parameterized by the control penalty R_2, where the point with the lowest state cost corresponds to the LQG controller with $R_2 = 10^{-10}$ (high-authority), while the point with the highest state cost correponds to the LQG controller with $R_2 = 10^{6}$ (low-authority). Associated with each curve are the asymptotic state cost and control cost of the adaptive controller. Since the target closed-loop dynamics are assigned to the asymptotic, high-authority LQG pole locations, the adaptive controller coincides with the high-authority LQG controller in each case.

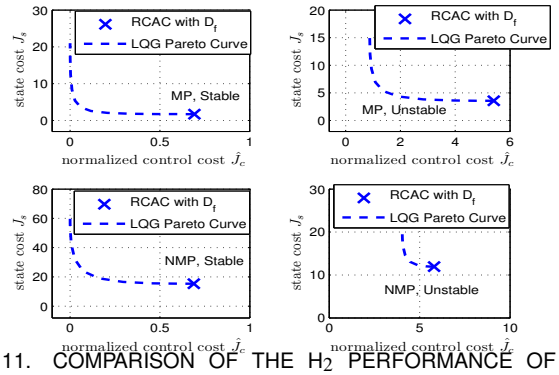

Figure 11. COMPARISON OF THE H_2 PERFORMANCE OF THE ASYMPTOTIC RCAC CONTROLLER UNDER LIMITED MODELING INFORMATION WITH THE LQG PERFORMANCE UNDER COMPLETE MODELING INFORMATION, FOR THE EXAMPLES CONSIDERED IN SECTIONS 6.1 AND 6.2. SINCE THE TARGET CLOSED-LOOP DYNAMICS ARE ASSIGNED TO THE HIGH-AUTHORITY LQG SYMMETRIC ROOT-LOCUS, THE ASYMPTOTIC ADAPTIVE CONTROLLER COINCIDES WITH THE HIGH-AUTHORITY LQG CONTROLLER IN EACH CASE.

7 CONCLUSION

Retrospective cost adaptive control (RCAC) was applied to an H_2 broadband disturbance rejection problem. The basic modeling information required is the first nonzero Markov parameter of the open-loop plant. Furthermore, it is shown through numerical examples that if the open-loop zeros of the plant are also known, the retrospective performance can be defined to allow RCAC recover the high-authority LQG performance. This is done by including the high-authority LQG closed-loop pole locations in the denominator of the filter which is used in the retrospective cost optimization. The configuration of these closed-loop poles can be determined by knowledge of only the open-loop zeros of the plant.

REFERENCES

[1] Dydek, Z. T., Annaswamy, A. M., and Lavretsky, E., 2010. "Adaptive Control and the NASA X-15-3 Flight Revisited: Lessons Learned and Lyapunov-stability-based Design". *IEEE Contr. Sys. Mag.,* **30**, pp. 32–48.

[2] Hovakimyan, N., Cao, C., Kharisov, E., Xargay, E., and Gregory, I. M., 2011. "L1 Adaptive Control for Safety-Critical Systems". *IEEE Contr. Sys. Mag.,* **31**, pp. 54–104.

[3] Astrom, K. J., and Wittenmark, B., 1995. *Adaptive Control*. Addison-Wesley.

[4] Goodwin, G. C., and Sin, K. S., 1984. *Adaptive Filtering, Prediction and Control*. Prentice Hall.

[5] Ioannou, P. A., and Sun, J., 1996. *Robust Adaptive Control*. Prentice Hall.

[6] Narendra, K. S., and Annaswamy, A. M., 1989. *Stable Adaptive Systems*. Prentice Hall.

[7] Kuo, S. M., and Morgan, D. R., 2011. "Active Noise Control: A Tutorial Review". *Proc. of the IEEE,* **87**(6), June, pp. 943–973.

[8] Patt, D., Liu, L., Chandrasekar, J., Bernstein, D. S., and Friedmann, P. P., 2005. "The Higher-Harmonic-Control Algorithm for Helicopter Vibration Reduction Revisited". *AIAA J. Guid. Contr. Dyn.,* **28**, pp. 918–930.

[9] Bodson, M., and Douglas, S. C., 1997. "Adaptive Algorithms for the Rejection of Sinusoidal Disturbances with Unknown Frequency". *Automatica,* **33**, pp. 2213–2221.

[10] Bodson, M., Jensen, J. S., and Douglas, S. C., 2001. "Active Noise Control for Periodic Disturbances". *IEEE Trans. Contr. Sys. Tech.,* **9**, pp. 200–205.

[11] Venugopal, R., and Bernstein, D., 2000. "Adaptive Disturbance Rejection Using ARMARKOV System Representation". *IEEE Trans. Contr. Sys. Tech.,* **8**, pp. 257–269.

[12] Hoagg, J. B., Santillo, M. A., and Bernstein, D. S., 2008. "Discrete-Time Adaptive Command Following and Disturbance Rejection with Unknown Exogenous Dynamics". *IEEE Trans. Autom. Contr.,* **53**, pp. 912–928.

[13] Iglesias, P. A., and Glover, K., 1991. "State-Space Approach to Discrete-Time H_∞ Control". *Int. J. of Contr.,* **54**, Nov., pp. 1031–1073.

[14] Prandini, M., and Campi, M. C., 2001. "Adaptive LQG Control of Input-Output Systems–A Cost-Biased Approach". *SIAM J. Contr. Optim.,* **39**(5), pp. 1499–1519.

[15] Daams, J., and Polderman, J. W., 2002. "Almost Optimal Adaptive LQ Control: SISO Case". *Math. Contr. Sig. Sys.,* **15**, pp. 71–100.

[16] Santillo, M. A., and Bernstein, D. S., 2010. "Adaptive Control Based on Retrospective Cost Optimization". *J. Guid. Contr. Dyn.,* **33**, pp. 289–304.

[17] Hoagg, J. B., and Bernstein, D. S., 2011. "Retrospective Cost Model Reference Adaptive Control for Nonminimum-Phase Discrete-Time Systems, Part 1: The Ideal Controller and Error System; Part 2: The Adaptive Controller and Stability Analysis". In Proc. Amer. Contr. Conf., pp. 2927–2938.

[18] D'Amato, A. M., Sumer, E. D., and Bernstein, D. S., 2011. "Frequency-Domain Stability Analysis of Retrospective-Cost Adaptive Control for Systems with Unknown Nonminimum-Phase Zeros". In Proc. Conf. Dec. Contr., pp. 1098–1103.

[19] Sumer, E. D., D'Amato, A. M., Morozov, A. M., Hoagg, J. B., and Bernstein, D. S., 2011. "Robustness of Retrospective Cost Adaptive Control to Markov Parameter Uncertainty". In Proc. Conf. Dec. Contr.

[20] Zhou, K., Doyle, J. C., and Glover, K., 1995. *Robust and Optimal Control*. Prentice Hall.

[21] Skogestad, S., and Postlethwaite, I., 1996. *Multivariable Feedback Control*. Wiley.

[22] Anderson, B. D. O., and Moore, J. B., 1989. *Optimal Control: Linear Quadratic Methods*. Prentice Hall.